Flowerlike ZnO Nanostructures via Hexamethylenetetramine-Assisted Thermolysis of Zinc−Ethylenediamine Complex

Xiangdong Gao,* Xiaomin Li, and Weidong Yu

State Key Laboratory of High Performance Ceramics and Superfine Microstructures, Shanghai Institute of Ceramics of Chinese Academy of Sciences, Shanghai, 200050, People's Republic of China

Received: August 19, 2004; In Final Form: September 27, 2004

Flowerlike ZnO nanostructures (FZNs) have been deposited on Si substrate from aqueous solution by the hexamethylenetetramine (HMT)-assisted thermolysis of zinc−ethylenediamine (en) complex at low temperature (95 °C) and in a short time (60 min). Obtained FZNs exhibit well-defined flowerlike morphology, hexagonal wurtzite structure, and strong UV photoluminescence. The flower petals constructed by many well-aligned nanorods possess the typical tapering feature with tip sizes of 30−50 nm. Effects of en, zinc−en molar ratio, HMT, and reaction time were investigated. Results show that en is determinative to the formation of FZNs, and the partial capping of $NH_3{\cdot}(CH_2)_2{\cdot}NH_3$ molecules on the side surface of the ZnO crystal is responsible for the tapering feature of petals. HMT can step into the nucleation process of ZnO and inhibit the formation of nanorods on the substrate by preventing heterogeneous precipitation. Moreover, the formation of twin crystal ZnO nuclei at low precursor concentrations and their further evolution into spindle crystals with clear middle interfaces are also vitally important for the development of FZNs.

Introduction

ZnO is one of the most important functional oxides with a direct, wide band gap (3.37 eV) and large excitation binding energy (60 meV), exhibiting many interesting properties including near-UV emission,[1] transparent conductivity,[2] and piezoelectricity.[3] The morphologically controllable synthesis of ZnO nanomaterials is spurred by the recent success in the realization of room-temperature UV lasing from a nanorod array by Yang et al.[4,5] Its great significance for the systematic fundamental study of structure−property relations and its wide variety of technological potentials as catalysts, selective separations, sensor arrays, waveguides, drug carriers, biomedical implants with macroporosity, and photonic crystals with tunable band gaps have inspired vast research interests.[6−16]

Up to now, well-defined ZnO nanostructures with an abundant variety of shapes, such as nanoneedles,[6] nanocables and nanotubes,[7] nanowalls,[8] nanobridges and nanonails,[9] nanohelixes, nanosprings, nanorings,[10−11] hierarchical nanostructures,[12] and mesoporous polyhedral cages and shells,[13] have been achieved through vapor-based techniques. Via the chemical solution route, tube-, tower-, and flowerlike ZnO nanostructures,[5,14−15] and oriented helical ZnO nanorod arrays[16] have also been realized very recently. However, despite great progress in this field, the shape-controlled synthesis of ZnO nanocrystals, especially regarding control over the complex structure, still remains a remarkable challenge. Recently, a significant advance in the morphologically controllable synthesis of ZnO has been made by Tian and co-workers,[17] based on their systematic modification of the crystal morphology of complex and oriented ZnO nanostructures. Their use of the seeded growth procedure to control the nucleation event and organic functional groups (citrate anions) to modify the mineral growth habit represents an important method to control formation of the complex nanostructures from the solution route. Therefore, it is both fundamentally interesting and technologically important to explore the effects of various organic additives on the nucleation and morphology of complex ZnO nanostructures.

Herein, we have extended Tian's concept by adopting hexamethylenetetramine (HMT), a highly water-soluble tetradentate cyclic tertiary amine, instead of spin-coated ZnO seeds, as the nucleation-control reagent and ethylenediamine (en), a strong bidentate chelating agent to zinc ions with a higher stability constant than other complexing agents such as ammonia or hydroxyl groups, as the capping reagent. According to its previous application in assembling new ligand−metal−ligand-type supramolecular architectures[18−20] and in fabricating ZnO nanorod arrays,[21,22] HMT is expected to release hydroxyl ions and act as the organic template at elevated temperature, thus dynamically modifying the nucleation process. Meanwhile, en is expected to influence the crystal growth habit of ZnO by both forming the complex precursor and capping the side face of the ZnO crystal.[23] In the present paper, by the joint use of HMT and en, the deposition of well-defined flowerlike ZnO nanostructures (FZNs) on Si substrate at low temperature (95 °C) and in a short reaction time (60 min) is successfully demonstrated. The crystallinity, morphology, and structure of FZNs are examined, and effects of the reaction conditions including the chelating agent en, zinc−en molar ratio, HMT, and reaction time are analyzed. Furthermore, from the angle of nucleation and morphology, the formation mechanism of FZNs will be discussed.

Experimental Section

All of the chemicals were analytic-grade reagents used without further purification. The aqueous precursor of the zinc−en complex was prepared by mixing zinc sulfate, en, and HMT at a molar ratio of 1:3:1 and zinc concentration of 0.001 mol/L. The precursor was poured into a laboratory Pyrex glass bottle with polypropylene autoclavable screw caps at a filling ratio of

* To whom correspondence should be addressed. E-mail address: xdgao@mail.sic.ac.cn. Phone: 86-021-52412441. Fax: 86-021-52413122.

10.1021/jp046267s CCC: $30.25
Published on Web 01/04/2005

TABLE 1: Sample Numbers, Reaction Conditions, and Obtained Morphologies

sample number	reaction media	heating rate (°C/min)	reaction time (min)	morphology
1	Zn/HMT/en = 1:1:3	4	60	flowerlike
2	Zn/HMT = 1:1, without en	4	60	sheetlike
3	Zn/HMT/en = 1:1:6	4	60	rod
4	Zn/en = 1:3, without HMT	4	60	flowerlike with rod
5	Zn/HMT/en = 1:1:3	4	6[a]	spindle
6	Zn/HMT = 1:1, without en, $[Zn^{2+}] = 0.0001$ M	1	60	rod

[a] After the occurrence of white precipitate in solution.

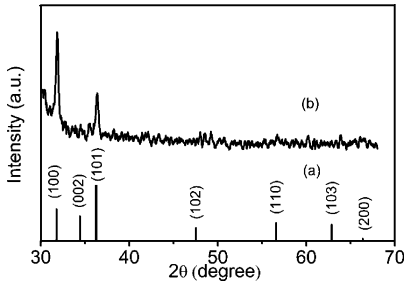

Figure 1. XRD patterns of (a) standard ZnO (JCPDS no. 36-1451) and (b) flowerlike ZnO.

80%. Si(111) wafers were placed in the bottom of the bottle for the harvest of products. The prepared precursor was heated from room temperature and maintained at the constant temperature of 95 °C for 1 h in a regular laboratory oven. Subsequently, the obtained white layer was thoroughly washed with pure water to eliminate the residual salts and organic substance and dried in air for subsequent measurements.

Five other similar experiments were also performed to examine the growth mechanism of FZNs. The first was without en, the second was without HMT, the third was at a lower zinc−en ratio (1:6), the fourth was at shorter reaction time (6 min after the appearance of white precipitate in solution), and the fifth was also without en but with a lower concentration of Zn^{2+} and lower heating rate. Table 1 gave the detailed reaction conditions of these experiments and morphologies obtained.

The structural and morphological characterization of the as-deposited sample was examined by D/max 2550V diffractometer (Rigaku Ltd., Japan, Cu Kα radiation), scanning electron microscope (SEM) (JSM-6700F), transmission electron microscopy (TEM) and electron diffraction (JEOL-2010). The photoluminescence spectra were measured by RF-5301PC fluorescence spectrophotometer (Shimadzu Ltd., Japan) at room temperature with an excitation wavelength of 340 nm. A Xe lamp with a filter was used as the excitation light source. For the TEM measurement, ZnO flowers were peeled from the substrate by a surgical knife and attached onto the copper grid for further analysis. For other measurements, the as-deposited sample on the substrate was used, and no additional treatment was required.

Results and Discussion

Structure and Morphology. Figure 1 shows X-ray diffraction patterns of standard ZnO (JCPDS no. 36-1451) and as-deposited ZnO layer on Si substrate. Results show that obtained FZNs possess the hexagonal wurtzite structure (space group $P6_3mc$) with good crystallinity, and no diffraction peaks of any other minerals were detected. In addition, different from either ZnO powder (Figure 1a) or FZNs in the powder form,[5,14] FZNs deposited on Si substrate exhibit two obvious diffraction peaks in the (100) and (101) planes, with higher intensity in the (100) plane. This means that the substrate can exert influence on the crystallographic behavior of FZNs.

Figure 2 illustrates SEM micrographs of FZNs on Si substrate. The low-resolution image (Figure 2a) shows that all ZnO flowers are 1−3 μm in size and are uniformly distributed on the substrate. The magnified SEM images in Figure 2b−d clearly reveal that obtained ZnO exhibits the well-defined flowerlike morphology. Three types of flowerlike morphology can be identified, that is, a flower cluster formed by accumulation of

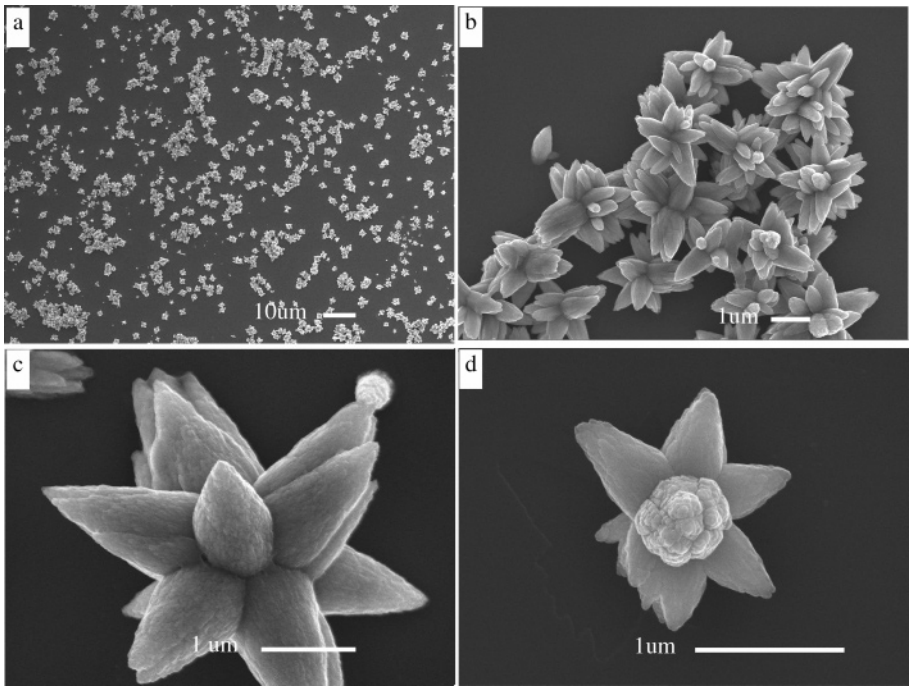

Figure 2. SEM micrographs of flowerlike ZnO structures: (a) low-resolution image, (b) ZnO flower cluster, (c) isolated ZnO flower with multilayer petals, and (d) isolated ZnO flower with monolayer petals.

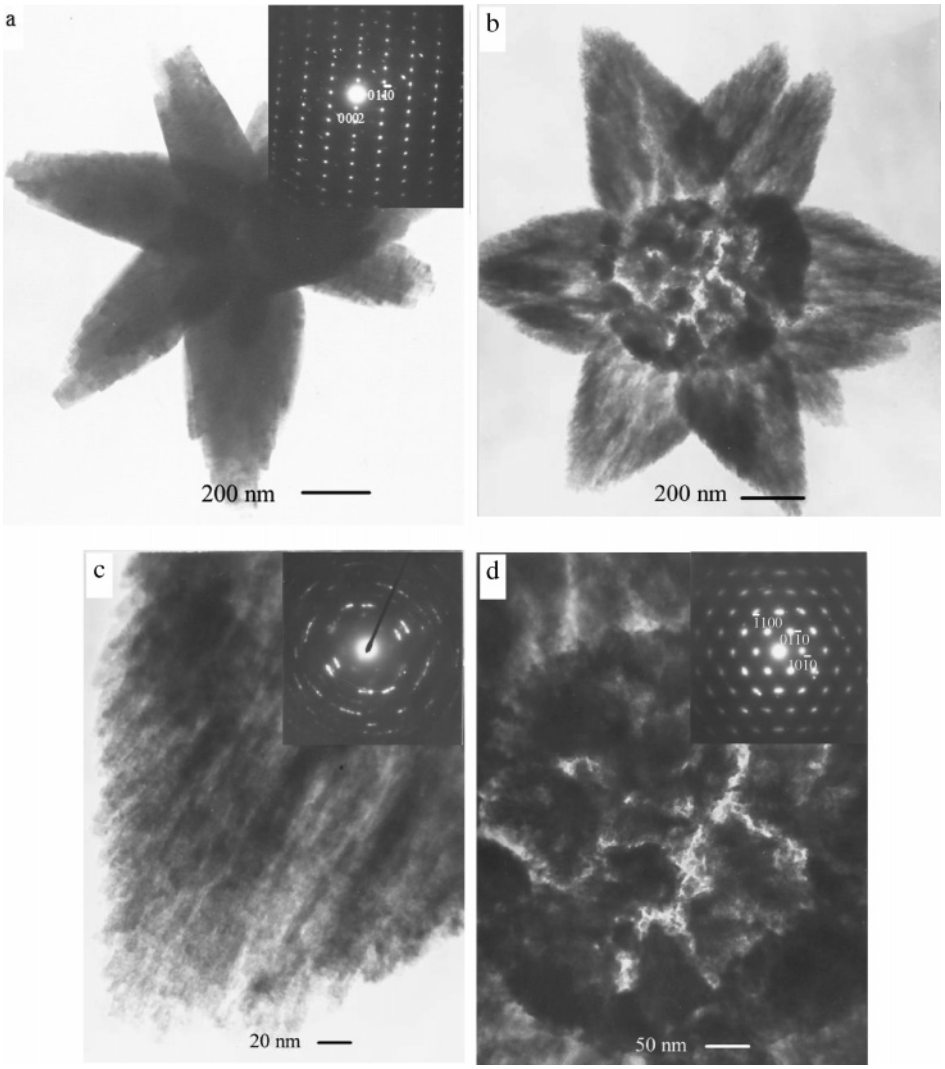

Figure 3. TEM micrographs of flowerlike ZnO structures: (a) ZnO flower formed at early period and SAED of one petal tip (inset), (b) ZnO flower formed at later period, (c) tip structure of one petal in (b) and its SAED pattern (inset), and (d) structure of style crystal in (b) and its SAED pattern (inset).

different flowers (Figure 2b), an isolated flower with multilayered petals (Figure 2c), and an isolated flower with a monolayer of petals (Figure 2d). Both the two types of isolated flower possess a similar configuration (i.e., an upstanding style crystal and some flatly lying petal crystals surrounding the style crystal). In contrast, for the flower cluster, usually no style crystal can be distinguished. Moreover, all the flower petals exhibit the tapering feature with the root size of 300−500 nm and tip size of 30−50 nm, on average, which is different from FZNs consisting of swordlike ZnO nanorods produced by the cetyltrimethylammonium bromide (CTAB)-assisted hydrothermal process.[14]

The deposition of FZNs is a time-dependent process (as will be discussed), and ZnO flowers formed at a different period may exhibit different structures. Figure 3a−d illustrates the representative TEM micrographs of two typical ZnO flowers and corresponding selective area electron diffraction (SAED) patterns. Figure 3a gives the structure of a typical ZnO flower with better crystallinity that may be formed in the earlier period and the SAED pattern of an individual petal crystal (inset). The tip structure of the petal shows that it is not a single-crystal rod but an assembly of several well-aligned nanorods. The SAED pattern indicates the single-crystal nature of a single nanorod and the growth direction along the (0002) plane. Figure 3b gives the structure of a ZnO flower with well-arranged petals and less crystallization, which may be formed in the later period. The magnified tip structure of the individual petal shown in Figure 3c illustrates that the petal is also built up by many well-aligned nanorods but with smaller diameter (∼5 nm), which possesses considerable similarity to the petal structure in Figure 3a. Correspondingly, the SAED pattern presented in the inset of Figure 3c is characterized by the symmetrical stripes rather than polycrystalline circles or arrayed spots, justifying the presence of some ordered arrangement of crystallites in the petal. Figure 3d presents the structure of the style crystal, which is located at the center of the petals and is probably grown parallel to the incidence direction of the electron beam. Results show that the style crystal is built up by several closely packed particles, and the strong and well-arrayed spots in the inset SAED pattern indicate the single crystalline nature of the individual component particle and the crystal growth along the (0002) plane.

Deposition Process. To provide a sound basis for the analysis of the growth mechanism of FZNs, the deposition process was analyzed on the basis of observed reaction phenomena occurring in the zinc−HMT−en tertiary system.

It is found that, for the zinc−HMT−en system, an induction period is required for the development of white precipitate after

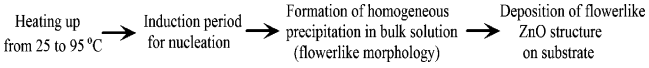

Figure 4. Schematic illustration of major reaction processes in the thermolysis of zinc−en complex assisted by HMT.

the solution temperature reaches 95 °C, and the duration of the induction period is dependent on the precursor concentration. A higher precursor concentration usually requires a longer induction period. After the induction period, a large quantity of white precipite will be formed in a few minutes. Analysis of the precipitated particles show that they exhibit the flowerlike morphology and good crystalline structure of ZnO, indicating that flowerlike ZnO is first formed in the bulk solution. However, precipitation in solution will not result in the immediate deposition of ZnO on the substrate. It is in the successive hydrothermal process that the suspended ZnO flowers in solution transform to FZNs on the substrate. A white layer on the substrate can be visibly detected after the hydrothermal reaction has been underway for about 20 min. When all the zinc ions in the precursor have been consumed (in about 60 min), the solution will become clear again. It can be inferred from the analysis on the deposition process that the deposition of FZNs on the substrate is in fact a time-dependent process, and nucleation on the substrate and crystal growth take place simultaneously. Therefore, two types of FZNs with different structures have been observed in Figure 3.

To determine the appropriate reaction time, the effect of longer reaction times, up to 15 h, has been investigated. Results show that reaction time exceeding 1 h will not bring about evident structural and morphological modifications. Therefore, a reaction time of 1 h is sufficient to obtain the well-defined FZNs. In comparison with other hydrothermal methods,[5,14,24] which usually require several hours or even days to obtain ZnO crystalline nanostructures, the method presented here is much more rapid and efficient. Figure 4 summarizes the major reaction processes occurring in the synthesis. Corresponding equations related to these processes are given as follows.

The zinc−en complex forms when the molar ratio of en to Zn^{2+} is higher than 3.

$$Zn^{2+} + 3NH_2{\cdot}(CH_2)_2{\cdot}NH_2 \leftrightarrow [Zn(NH_2{\cdot}(CH_2)_2{\cdot}NH_2)_3]^{2+} \quad (1)$$

At elevated temperature (up to 95 °C in this experiment), the chemical equilibrium in eq 1 moves to the left and the zinc−en complex decomposes, resulting in the increase of Zn^{2+} concentration.

Meanwhile, OH^- concentration increases because of the hydrolysis of both HMT and en.

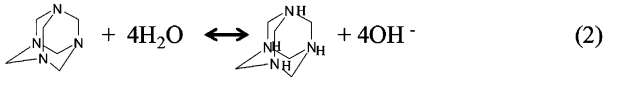

(2)

$$NH_2{\cdot}(CH_2)_2{\cdot}NH_2 + 2\,H_2O \leftrightarrow NH_3{\cdot}(CH_2)_2{\cdot}NH_3 + 2OH^- \quad (3)$$

Thus, $Zn(OH)_2$ and ZnO will be formed under the hydrothermal condition by

$$Zn^{2+} + 2OH^- \rightarrow Zn(OH)_2 \rightarrow ZnO + H_2O \quad (4)$$

It can be seen from this analysis that two types of organic molecules are present in the reaction system (i.e., $NH_3{\cdot}(CH_2)_2{\cdot}NH_3$ (abbreviated as en−H2) and hydrolyzed HMT (abbreviated as HMT−H4)). To explore the root cause for the development of the flowerlike morphology, the functions of these two organic substances have to be understood.

Effects of en. To examine the function of en in the deposition process of FZNs, the morphologies of two control samples without en (sample **2**) and with lower zinc−en ratio (1:6, sample **3**) were compared with sample **1**. Figure 5a,b illustrates SEM images of the ZnO structure in samples **2** and **3**.

When only HMT was used as the supplier of OH^- and no en was added, $Zn(OH)_2$ nanosheet rather than flowerlike ZnO was obtained (Figure 5a). When en was used with a zinc−en ratio of 1:3, which means that the amount of en is just enough to complex all the zinc ions in the precursor and form a clear precursor solution, clearly defined ZnO flowerlike structures were obtained, and almost all petal crystals exhibit a tapering feature, as illustrated in Figure 2. When en was excessive to Zn^{2+} and the zinc−en ratio was 1:6, only isolated ZnO rods and a few sparsely distributed irregular aggregations of ZnO rods, rather than FZNs, were obtained (Figure 5b). In addition, all the obtained ZnO rods in sample **3** exhibit smaller diameter, higher aspect ratio, and much less tapering feature. These results indicate that the chelating agent en and proper zinc−en ratio are key factors for the formation of FZNs.

ZnO crystal is a polar crystal whose positive polar plane is rich in Zn and negative polar plane is rich in O. In the hydrothermal process, the negative nature of the growth unit $[Zn(OH)_4]^{2-}$ will lead to the different growth rates of planes, that is, $V_{(0001)} > V_{(10\bar{1}\bar{1})} > V_{(\bar{1}010)} > V_{(\bar{1}011)} > V_{(000\bar{1})}$. When there is no organic additive in solution, spherical ZnO particles will be easily developed because of the Ostwald ripening process.[25] When en is present in the aqueous solution, en will hydrolyze and form en−H2 according to eq 3, which bears two positive charges. Thus, by the coulomb interaction, en−H2 molecules will adsorb on the negative polar planes (i.e., (1011), (1010), and (1011) planes) retarding the growth rate of these planes. Therefore, the concentration of en in the precursor has significant effects on the morphology of ZnO crystals. When the concentration of en is high enough, en−H2 molecules will cover all the side surfaces of the ZnO crystal, thus enhancing the growth along the (0002) plane greatly and resulting in the formation of rods with uniform diameters and high aspect ratios. However, when the concentration of en is relatively low, there will not be enough en−H2 molecules to cover all the side surfaces of ZnO crystal. So, both the impeding effect of en on the crystal growth and the Ostwald ripening process will take effect, thus resulting in the formation of petal crystals with the obvious tapering feature.

Effects of HMT. To examine the function of HMT in the formation of FZNs, morphologies of sample **4** without HMT were compared with those of sample **1**. When no HMT was used, as shown in Figure 5c, many ZnO rods with diameters of 200−300 nm were grown on the substrate apart from the flowerlike structures. These ZnO rods may originate from the heterogeneous deposition of ZnO on the Si substrate at the initial stage of thermolysis of the zinc−en complex. When HMT was used, as can be seen from Figure 2a, almost all the deposited ZnO particles possess the flowerlike morphology, and very few ZnO rods were formed. So, HMT can inhibit the formation of undesired nanorods on the substrate effectively. During the heating process to 95 °C, HMT will hydrolyze and release OH^- into solution by eq 2, leading to the increase of both the concentration of OH^- and the ionic product of $Zn(OH)_2$. So, the heterogeneous precipitation of $Zn(OH)_2$ on the substrate, which requires lower ionic product than the homogeneous

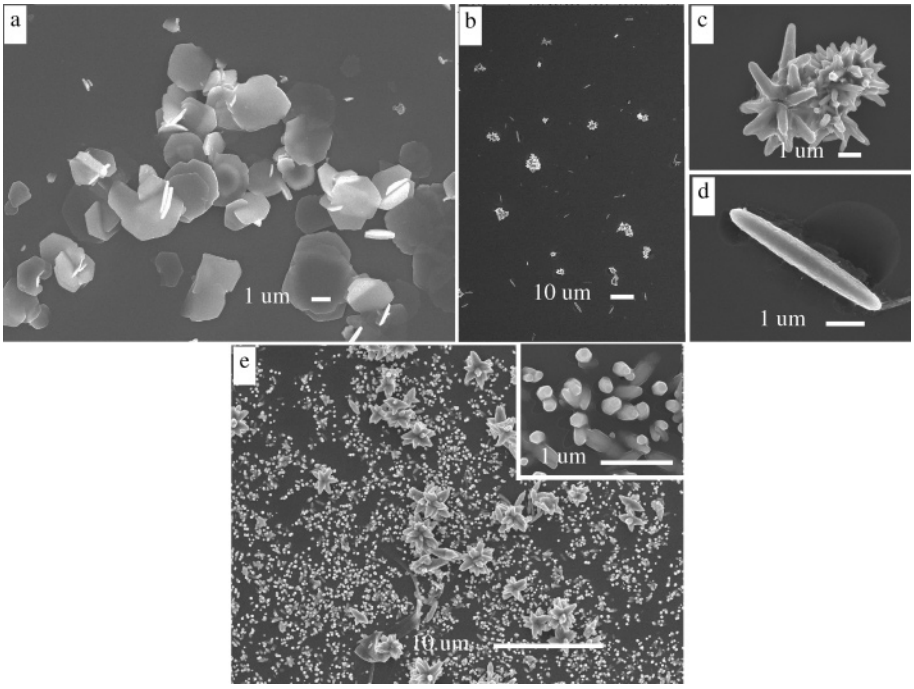

Figure 5. SEM micrographs of ZnO structures with different precursors: (a) zinc−HMT ratio of 1:1 without en, (b) low-resolution image of ZnO structure with zinc−HMT−en ratio of 1:1:6, (c) irregular aggregation of ZnO rods in (b), (d) individual ZnO rod in (b), and (e) zinc−en ratio of 1:3 without HMT, and the inset is a closeup view of nanorods in (e).

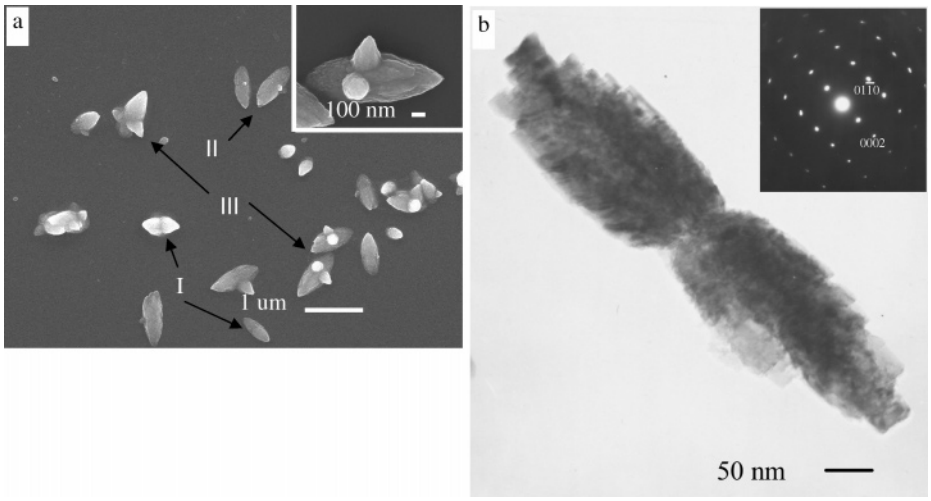

Figure 6. SEM (a) and TEM (b) micrographs of ZnO structure obtained after reaction time of 6 min after the induction period. Three types of ZnO particles were identified: type I, spindle crystals with a middle interface; type II, spindle crystals with one budding petal; and type III, spindle crystals with two budding petals. The inset of (a) is a closeup view of a typical type III particle. (b) TEM image of type I particle and its SAED pattern (inset).

precipitation, can be effectively prevented in the initial stage of the thermolysis process.

Moreover, it has been reported that infinite chains of $[Zn(HMT)Cl_2]_n$ can be formed by didentate coordination linking tetrahedral zinc ions.[18,19] So, it is reasonable to believe that a similar complex structure may exist in the current zinc−HMT−en system as well. First, the structure can act as the nucleation center and facilitate the homogeneous precipitation of $Zn(OH)_2$ in the bulk solution. Second, it can serve as the organic template and modify the nucleation process and resultant structure of ZnO. It has been reported that, under the hydrothermal condition, HMT can promote the formation of well-aligned and highly crystallized ZnO nanorods and nanowires when the ZnO seed layer was adopted.[18−19,26−27] In our experiment, it is also expected that HMT will promote the formation of nanorods constituting the petal crystal of the flower. Third, HMT−H4 molecules may also help to form twin crystal ZnO nuclei during the nucleation process, as will be discussed in the following section.

Morphologies Arrested at Early Reaction Period. Because the deposition of FZNs is a time-dependent process, as mentioned already, ZnO structures formed at a different period can be effectively arrested in one sample. Therefore, we have examined the morphology of ZnO structures deposited at the early reaction period (sample **5**), as shown in Figure 6, with the intent to further probe the initial growth process of FZNs. Three types of ZnO structures with different morphologies can be identified in Figure 6a: the spindle crystal joined by two elongated connoids at the bottom with a junction interface in the middle part (type I), spindle crystal with only one budding petal deposited at the junction interface (type II), and spindle crystal with two or more developing petals at the junction

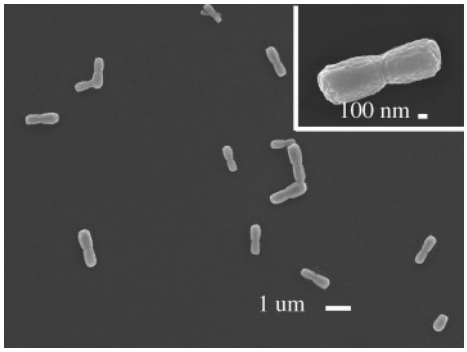

Figure 7. SEM micrograph of ZnO structure with low precursor concentration ($[Zn^{2+}] = 0.0001$ mol/L), zinc−HMT ratio of 1:1, and without en. The inset is a closeup view of an individual ZnO rod exhibiting a clear interface at the middle .

interface (type III). Figure 6b gives the TEM image of a typical ZnO spindle and its SAED pattern. The steplike fringe in the petal tip structure indicates that the spindle is also built up by several well-aligned ZnO nanorods. The inset SAED pattern reveals that the nanorods constituting the spindle are single-crystal and that the growth is along the (0002) plane. These results support the supposition that, prior to the development of petal crystals, the spindle crystal with an interface at the middle part will be formed first.

The formation of the spindle crystal with a middle interface is vitally important for the development of FZNs. To get a better understanding of its formation mechanism, the actual nucleation condition was simulated in the zinc−HMT system by lowering the precursor concentration and the release rate of OH^-. To eliminate the capping effects of en−H2 molecules, en was not used in this simulated experiment. The detail reaction conditions were given in Table 1 (sample **6**), and the morphology of obtained ZnO structure was illustrated in Figure 7. Results show that obtained ZnO exhibits the typical rod structure with an aspect ratio of 4−5 and diameter of 500 nm. Especially, all ZnO rods possess similar features to the flower petal (i.e., the relatively smaller diameter at the middle part of the rod and a clear middle interface). When other conditions are maintained but the Zn^{2+} concentration increased, the rod diameter increases and the height decreases, resulting in the sheetlike structure (just like the morphology in Figure 5a) rather than rods. Therefore, the low precursor concentration in the reaction system may be an important factor responsible for the formation of spindles with the middle interface. In the zinc−HMT−en system, the very low concentration of Zn^{2+} can be achieved by the slow decomposition of the zinc−en complex in the initial period. In the mechanism, the spindle crystals or rods with a middle interface should originate from the twin crystal ZnO nuclei. The organic additive HMT may be helpful for the formation of twin crystal ZnO nuclei by providing templates for the nucleation and the orientation growth of ZnO crystals. But, it is not absolutely necessary, because similar FZNs can also be obtained when only en was used (sample **4**), and similar rod structures have also been observed in the hydrothermal process of $[Zn(OH)_4]^{2-}$ for the reaction time of 10 min by J. Zhang et al.[5] Obviously, further investigation on this phenomenon is still needed.

Growth Mechanism. On the basis of these experimental results and analysis, the formation mechanism of FZNs can be outlined as follows: With the decomposition of $[Zn(en)_3]^{2+}$ complex and the hydrolysis of en and HMT at elevated temperature, the concentrations of Zn^{2+} and OH^- increase correspondingly, and $Zn(OH)_2$ and/or ZnO nuclei start to form when the degree of supersaturation exceeds the critical value. In the hydrothermal process, twin crystal ZnO nuclei will be developed under the low precursor concentration and the action of HMT−H4, forming spindle crystals with a middle interface. Because of the higher surface energy at the middle interface of spindle crystals, en−H2 molecules released from the decomposition of $[Zn(en)_3]^{2+}$ will adsorb on the interface first, resulting in a decrease of the surface energy and the generation of active sites. The active sites will trigger the nucleation at the interface, promoting the formation of petal crystals extending from the interface. In view of the symmetry involved in the crystal growth process, the petal crystals will be uniformly distributed around the style crystal (one of the initially formed twin crystal), thus forming the well-defined flowerlike ZnO structure. In addition, en−H2 molecules can also adsorb on the side surface of twin crystal ZnO nuclei by coulomb action and form the partial capping of en−H2 molecules on ZnO crystal due to the low en−zinc molar ratio in the precursor. Therefore, the petal crystals with the tapering feature were finally developed. Figure 8 shows the growth schematic diagram of FZNs in the zinc−HMT−en tertiary system.

Photoluminescence. The obtained FZNs possess petal crystals with the distinguished tapering feature, whose tip size is on the order of 30−50 nm. This novel micro-nanohybrid structure may exhibit fancy optical and electrical properties, which may find vast applications as the photoelectrical component in potential nanodevices or as special catalyst support, and so on. Figure 9 illustrates the photoluminescence spectrum of the flowerlike ZnO structure under photon excitation of 340 nm. A strong and sharp UV emission at 389 nm dominates the photoluminescence spectrum, with several weak emission peaks in the blue and blue-green bands (449, 467, 481, and 493 nm). In particular, the UV emission peak is well-fitted with two Gaussian peaks (thinner lines in the inset), that is, a broad peak from 365 to 420 nm and a sharp peak from 384 to 393 nm. Moreover, the narrow and intense UV peak exhibits a fwhm of about 5.4 nm, which is much smaller than the values of a ZnO single-crystal nanorod,[28] ZnO nanoneedle,[6] and ZnO flowers.[5] This particular UV emission behavior may be related to the flowerlike morphology and the special petal structures in the obtained sample. As for the mechanism, it is commonly accepted that the UV emission should be attributed to the radiative

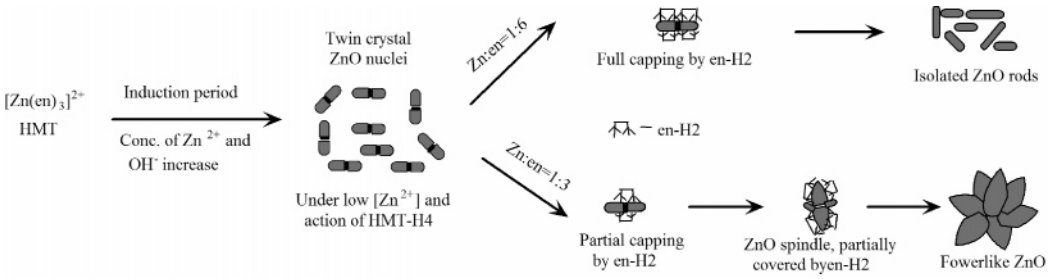

Figure 8. Schematic diagram of the growth mechanism of flowerlike ZnO nanostructures in the zinc−HMT−en tertiary system.

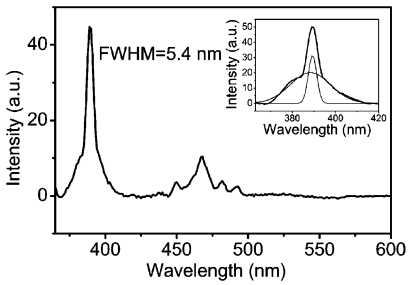

Figure 9. Photoluminescence spectrum of flowerlike ZnO structures under the photon excitation of 340 nm at room temperature. Inset gives the detail spectrum of UV emission and two fitted Gaussian peaks (thinner lines).

annihilation of excitons,[29−30] and the weak peaks in the blue-green band may originate from the electron transition from the level of the ionized oxygen vacancies to the valence band.[31] The sharp and intense UV emission, the weak emission related to ionized oxygen vacancies, and the absence of the well-known stronger and broader emission in the yellow-green band illustrate the good crystallization quality and high stoichiometric nature of the obtained products.

Conclusion

A novel and rapid thermolysis method of the zinc−en complex mediated by HMT was proposed to fabricate ZnO nanostructures with well-defined flowerlike morphologies. The flower petals built up by many well-aligned nanorods are in the typical tapering feature with tip sizes of 30−50 nm. The overall FZNs exhibit hexagonal wurtzite structure, strong UV emission, and uniform distribution on the substrate. While HMT mediates the nucleation and growth of ZnO crystals by modifying the solution basicity and providing organic templates, the chelating agent en and the zinc−en molar ratio have determinative effects on the formation of FZNs. The tapering feature of petals is mainly due to the partial capping of $NH_3 \cdot (CH_2)_2 \cdot NH_3$ molecules on the side surface of the ZnO crystal. A special spindle with an interface at the middle will be formed first, and the petal crystals subsequently nucleate and develop at the interface because of its higher surface energy. Further investigation shows that the specific spindle structure may be closely related to the formation of twin crystal ZnO nuclei under the low precursor concentration. This paper provided a novel and simple solution route to prepare ZnO nanostructures with complex morphologies through control of the nucleation event by organic additives and modification of the crystal growth habit by capping reagents, which will be expected to find vast applications in the morphological synthesis of other similar oxide nanocrystals.

Acknowledgment. This work is financially supported by the Ministry of Science and Technology of China through the 973-project under grant no. 2002CB613306.

References and Notes

(1) Service R. F. *Science* **1997**, *276*, 895.
(2) *MRS Bull.* **2000**, *8*, August issue (special issue on transparent conducting oxides).
(3) Minne, S. C.; Manalis, S. R.; Quate, C. F. *Appl. Phys. Lett.* **1995**, *67*, 3918.
(4) Huang, M. H.; Mao, S.; Feick, H.; Yan, H. Q.; Wu, Y. Y.; Kind, H.; Russo, R.; Yang, P. D. *Science* **2001**, *292*, 1897.
(5) Zhang, J.; Sun, L.; Yin, J.; Su, H.; Liao, C.; Yan, C. *Chem. Mater.* **2002**, *14*, 4172.
(6) Park, W. I.; Yi, G. C.; Kim, M.; Pennycook, S. J. *Adv. Mater.* **2002**, *14*, 1841.
(7) Hu, J. Q.; Li, Q.; Meng, X. M.; Lee, C. S.; Lee, S. T. *Chem. Mater.* **2003**, *15*, 305.
(8) Lao, J. Y.; Huang, J. Y.; Wang, D. Z.; Ren, Z. F.; Steeves, D.; Kimball, B.; Porter, W. *Appl. Phys. A* **2004**, *78*, 539.
(9) Lao, J. Y.; Huang, J. Y.; Wang, D. Z.; Ren, Z. F. *Nano Lett.* **2003**, *3*, 235.
(10) Kong, X. Y.; Wang, Z. L. *Nano Lett.* **2003**, *3*, 1625.
(11) **(**11) Kong, X. Y.; Ding, Y.; Yang, R.; Wang, Z. L. *Science* **2004**, *303*, 1348.
(12) Lao, J. Y.; Wen J. G.; Ren, Z. F. *Nano Lett.* **2002**, *2*, 1287.
(13) Gao, P. X.; Wang, Z. L. *J. Am. Chem. Soc.* **2003**, *125*, 1299.
(14) Zhang, H.; Yang, D.; Ji, Y.; Ma, X.; Xu, J.; Que, D. *J. Phys. Chem. B.* **2004**, *108*, 3955.
(15) Wang, Z.; Qian, X. F.; Yin, J.; Zhu, Z. K. *Langmuir* **2004**, *20*, 3441.
(16) Tian, Z. R.; Voigt, J. A.; Liu, J.; McKenzie, B.; McDermott, M. J. *J. Am. Chem. Soc.* **2002**, *124*, 12954
(17) Tian, Z. R.; Voigt, J. A.; Liu, J.; McKenzie, B.; McDermott, M. J.; Rodriguez, M. A.; Konishi, H.; Xu, H. F. *Nat. Mater.* **2003**, *2*, 821.
(18) Pickardt, J.; Droas, P. *Acta Crystallogr., Sect. C* **1989**, *45*, 360.
(19) Zheng, S. L.; Tong, M. L.; Chen, X. M. *Coord. Chem. Rev.* **2003**, *246*, 185.
(20) Erxleben, A. *Coord. Chem. Rev.* **2003**, *246*, 203.
(21) Vayssieres, L. *Adv. Mater.* **2003**, *15*, 464.
(22) Boyle, D. S.; Govender, K.; O'Brien, P. *Chem. Commun.* **2002**, 80.
(23) Liu, B.; Zeng, H. C. *J. Am. Chem. Soc.* **2003**, *125*, 4430.
(24) Cheng, B.; Samulski, E. T. *Chem. Commun.* **2004**, 986.
(25) Marqusee, J. A.; Ross, J. *J. Chem. Phys.* **1983**, *79*, 373.
(26) Gorender, K.; Boyle, D. S.; O'Brien, P.; Binks, D.; West, D.; Coleman, D. *Adv. Mater.* **2002**, *14*, 1221.
(27) Choy, J. H.; Jang, E. S.; Won, J. H.; Chung, J. H.; Jong, D. J.; Kim, Y. W. *Adv. Mater.* **2003**, *15*, 1911.
(28) Guo, L.; Ji, Y. L.; Xu, H. *J. Am. Chem. Soc.* **2002**, *124*, 14864.
(29) Monticone, S.; Tufeu, R.; Kanaev, A. V. *J. Phys. Chem. B* **1998**, *102*, 2854.
(30) Dijken, V. A.; Meulenkamp, E. A.; Vanmaekelbergh, D.; Meijerink, A. *J. Lumin.* **2000**, *87*−*89*, 454.
(31) Zhang, D. H.; Wang, Q. P.; Xue, Z. Y. *Appl. Surf. Sci.* **2003**, *207*, 20.